Earth, Planets and Space

FULL PAPER Open Access

Dispersal and grain size characteristics of the May 14, 2018 Shinmoedake eruption deposit, Kirishima Volcano, Japan, based on post-eruption field survey and meteorological datasets

Yasuo Miyabuchi[1*] and Eiichi Sato[2]

Abstract

This study describes the dispersal and grain size characteristics of the May 14, 2018 Shinmoedake eruption deposits of Kirishima Volcano in southern Kyushu, southwestern Japan. We discuss the eruption sequence, including the temporal variations in the behavior of the plume, by combining field and meteorological datasets. Following a magmatic activity in 2011 characterized by a substantial change in the eruption style (from subplinian eruptions to lava effusion) and subsequent vulcanian explosions, the Shinmoedake crater experienced intermittent eruptions in 2018. The May 14, 2018 eruption began at 14:44 with a vulcanian eruption, with the eruption plume rising 4500 m above the crater rim. Thereafter, it transitioned to an ash eruption; the plume height decreased gradually until the eruption ceased at 16:10. The tephra fall deposits were distributed more than 27 km to the southeast of the source crater; the mass of the tephra fall deposit was approximately 2.1×10^7 kg, calculated based on an isomass map. The deposit incidence differed between the east and west sides of the major dispersal axis. The deposits found east of the main dispersal axis were primarily composed of coarse to medium sand-sized particles with no fine fraction (fine sand to silt in size). In contrast, the deposits west of the axis were finer-grained than those east of the axis. We analyzed photographs of the eruption plume, along with the regional meteorological data and the dispersal and grain-size characteristics of the deposits, and reached the following conclusion: during the May 14, 2018 eruption, the wind directions above the Shinmoedake crater fluctuated across altitudes. The westerly winds dispersed the eruption plume that rose to a higher altitude, containing coarser tephra associated with the initial vulcanian eruption, further to the east rather than along the main axis. In contrast, a lower-altitude ash eruption plume that was rich in fine materials was dispersed westward rather than along the main axis, which was influenced by northerly winds. The findings of this study can support the analysis of similar volcanic events.

Keywords Dispersal characteristics, Erupted mass, Eruption plume, Grain size, Kirishima Volcano, Meteorological conditions, Shinmoedake, Tephra fall

*Correspondence:
Yasuo Miyabuchi
miyabuchi@gmail.com
Full list of author information is available at the end of the article

Graphical Abstract

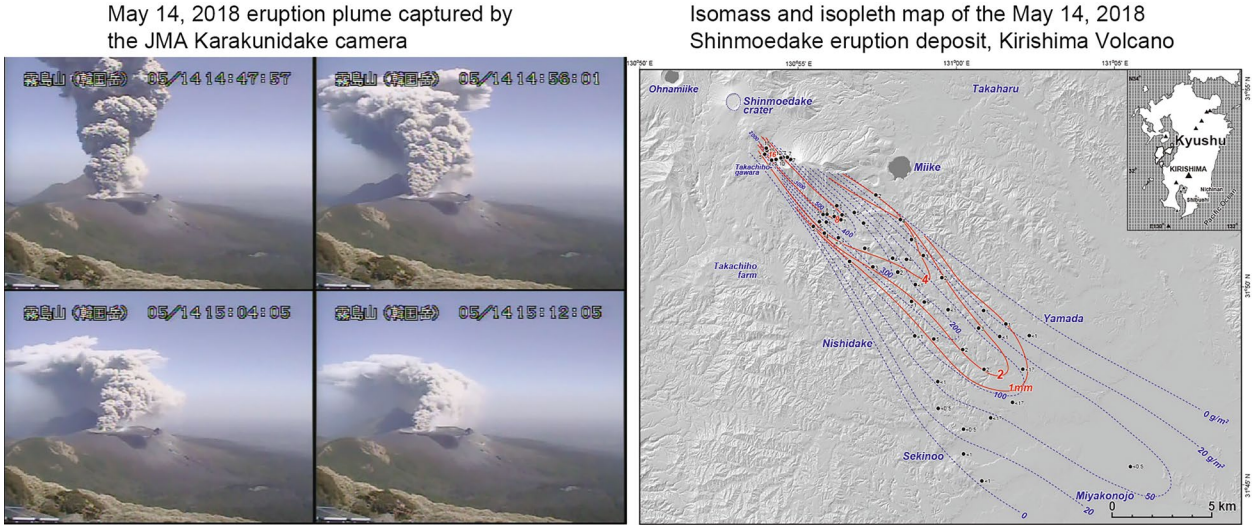

Introduction

In addition to the eruption style, column height, and duration, meteorological conditions, such as wind direction and speed, as well as the differences in the characteristics of the plume at different altitudes, have a substantial impact on the dispersal of fallout tephra (Poulidis et al. 2018). Tephra falls pose threats to the local population and could damage the surrounding infrastructure and agricultural land. Therefore, one of the most crucial challenges in volcanology is anticipating tephra dispersion during volcanic eruptions to clarify their influence and mitigate the related disasters. In recent years, weather radar data have been used to evaluate the behavior of eruption plumes and tephra dispersal (Hashimoto et al. 2012; Shimbori et al. 2013; Sato et al. 2018; Sato 2021). To validate such methodologies, the tephra fall distribution and grain-size data obtained in the field should be compared with meteorological data; however, the studies that have applied this process are limited.

On May 14, 2018, the Japan Meteorological Agency (JMA) captured web-camera photographs of the eruption plumes, along with the meteorological data, including the wind directions and speeds at different altitudes of the Shinmoedake eruption at Kirishima Volcano (southern Kyushu, southwestern Japan). We conducted fieldwork immediately after the eruption to sample and examine the tephra fall deposits. In this report, we present the distribution, discharged mass, and grain-size characteristics of the related deposits. In addition, we discuss the eruption sequence, including the temporal variations in the behavior of the eruption plume, using a combination of field and meteorological datasets.

Shinmoedake Volcano and the eruption in 2018

Kirishima Volcano is a Quaternary composite volcano located in southern Kyushu, southwestern Japan. It spans approximately 30 km from east to west and 25 km from north to south and includes a cluster of more than 25 small andesitic stratovolcanoes and two calderas (Imura 1994; Imura and Kobayashi 2001). Shinmoedake (1420.8 m above the sea level: ASL), located near the center of the Kirishima Volcano, is an andesitic stratovolcano consisting of a crater (approximately 800 m in diameter) at the summit. It became active with the Setao pumice fall (Inoue 1988) that occurred in 10.4 cal ka BP (calibrated ^{14}C date from Imura and Koga (1992)) and has continuously experienced intermittent small eruptive episodes (5.6 cal ka BP; AD 1716-1717; AD 1959). The 1716-1717 Kyoho eruption was the largest eruption of the Shinmoedake Volcano, consisting of large pumice-fall and pyroclastic flow deposits. The majority of the current volcanic edifices of the Shinmoedake Volcano are believed to have been formed by the Kyoho eruption.

A series of eruptions at Shinmoedake Volcano in 2011 was characterized by a significant change in the eruption style (from subplinian eruptions to lava effusion)

in the summit crater, followed by vulcanian eruptions (Kozono et al. 2013; Nakada et al. 2013; Miyabuchi et al. 2013). Small eruptions that produced ash falls followed in October 2017 (Fukuoka Regional Headquarters and Kagoshima Meteorological Office 2018). The 2018 eruptions from the Shinmoedake crater began on March 1, and the ash emissions lasted until March 9. New lava flows continued to discharge in the summit crater during March 6–9 and then, on March 9, the effusive eruptions flowed northwest outside the crater. The 34 vulcanian eruptions occurred on March 6 and 7, 2018. Several vulcanian eruptions occurred on March 10 and 25 and April 5, 2018, and slow lava flows (flow width: ~ 200 m) were observed after March 9, 2018. Ballistic clasts (found at a distance of 800–1000 m from the center of the crater) and minor pyroclastic density currents (PDCs) (found at a distance of < 400 m from the center of the crater) were produced by the eruptions that occurred on March 10 and April 5 (Fukuoka Regional Headquarters and Kagoshima Meteorological Office 2019).

On May 14, 2018, the eruption began at 14:44 (Japan Standard Time: JST; GMT + 9 h) and ceased at 16:10. The eruptive event can be divided into two stages. The event initially began with a vulcanian eruption and quickly transitioned to the ash-emission stage, continuing until 16:10. The plume of the vulcanian eruption rose to an altitude of at least 4500 m above the crater rim (approximately 5900 m ASL) at 14:50 and then dispersed to the southeast. Although no ballistic clasts or PDCs were found near the crater, ash fall on the road surface and small lapilli (< 7 mm in long-axis diameter) were observed approximately 7 km southeast of the crater. The distal ash extended to the Nichinan (60 km SE) and Shibushi (50 km SSE) cities along the Pacific coast (Fukuoka Regional Headquarters and Kagoshima Meteorological Office 2019). The JMA observed an infrasound of amplitude 3.3 Pa at the Yunono site located 2.7 km southwest of the Shinmoedake crater (Fig. 1). The JMA defines the explosions at Kirishima Volcano as eruptions accompanied by explosion earthquakes having an infrasound amplitude of at least 20 Pa at the Yunono observation site; therefore, the May 14, 2018 eruption was not considered to be explosive.

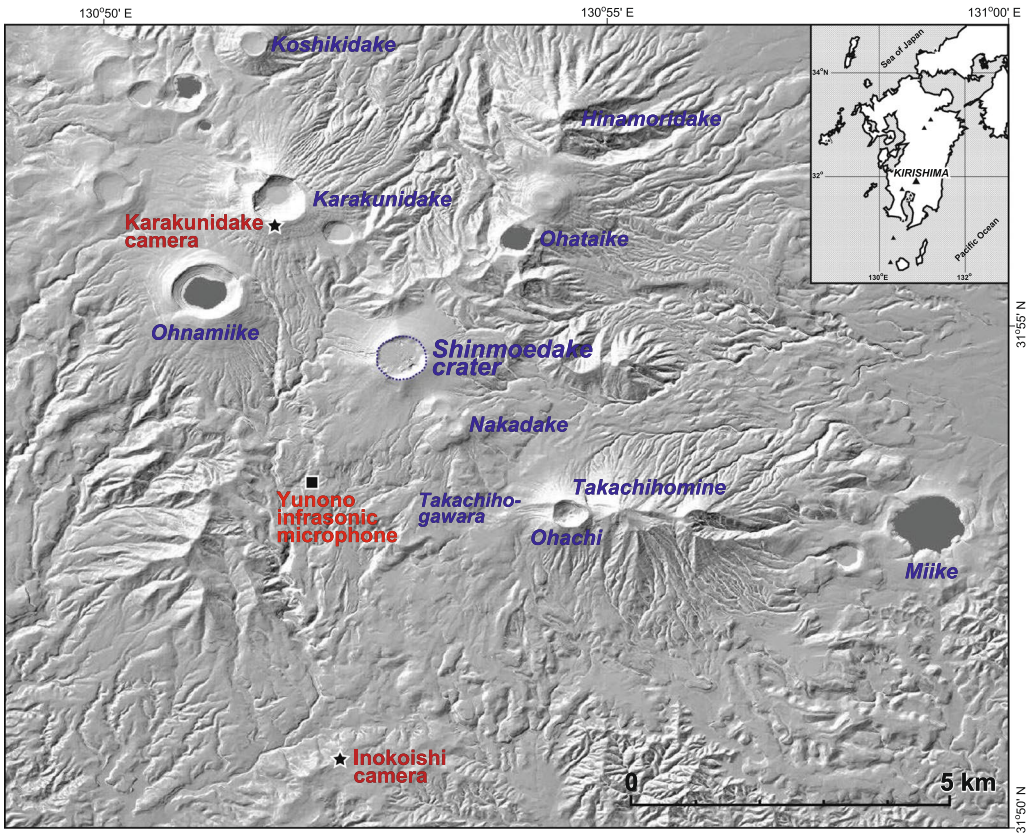

Fig. 1 Location of observation sites (cameras and infrasonic microphone) installed by the Japan Meteorological Agency (JMA) in Kirishima Volcano. The relief map was produced by the Kashmir 3D software, using the 10-m-mesh digital elevation model (DEM) data published by the Geospatial Information Authority of Japan

On June 22, there was a vulcanian explosion consisting of ballistics (found more than 1100 m from the crater), followed by a minor eruption with an ash plume rising 2200 m above the crater rim (~3600 m ASL) on June 27. No other eruptions occurred until the end of 2018. The eruptions that occurred from October 2017–June 2018 at Shinmoedake Volcano can be divided into three phases: phreatic/phreatomagmatic explosion (October 11, 2017–March 5, 2018), lava dome formation with weak explosion (March 6–8, 2018), and vulcanian explosion (March 8–June 27, 2018) (Maeno et al. 2023).

Methods

First, we carried out fieldwork and surveys in and around Kirishima Volcano on May 15–16 and June 13, 2018, to examine the tephra deposits associated with the May 14, 2018 eruption of Shinmoedake Volcano. We observed tephra deposits at 58 locations southeast of the Shinmoedake crater, extracted tephra samples at 50 sites from the surfaces of manufactured constructions, including roadways and concrete floors, and measured the area from which the samples were collected (Additional file 1: Table S1). In addition, we recorded the maximum size of the lithic fragments (ML; average long-axis diameter of the three largest lithic clasts) at each locality. The most proximal site was located approximately 3 km southeast of the Shinmoedake crater, and the most distant site was located approximately 26 km southeast of the crater (Fig. 2). We dried the samples and measured their masses, and then calculated the mass loading/m^2 (g/m^2) for each sampling point. An isomass distribution map was drawn based on the mass loading/m^2 data at each sampling point. The discharged mass for the May 14, 2018 eruption deposit was calculated using the method described in the following section.

Deposits from the eruption on May 14, 2018, were mechanically sieved for grain size analysis. The samples were dried and sieved from −3 to 5 ϕ (8–1/32 mm), at 1 ϕ intervals. The median diameters (Md_ϕ), Inman's (1952) sorting coefficients (σ_ϕ) and the Walker (1983) parameters of F1 (weight percentage finer than 1 mm) and F2 (weight percentage finer than 1/16 mm) were calculated (Additional file 2: Table S2). Because the most predominant grain size fractions in the majority of tephra samples were 1–2 ϕ or 0–1 ϕ (1/2–1 mm), we studied the ash grains in the fractions 1–2 ϕ (1/2–1/4 mm, generally washed ultrasonically) using a digital microscope (Leica DMS1000), to determine their components.

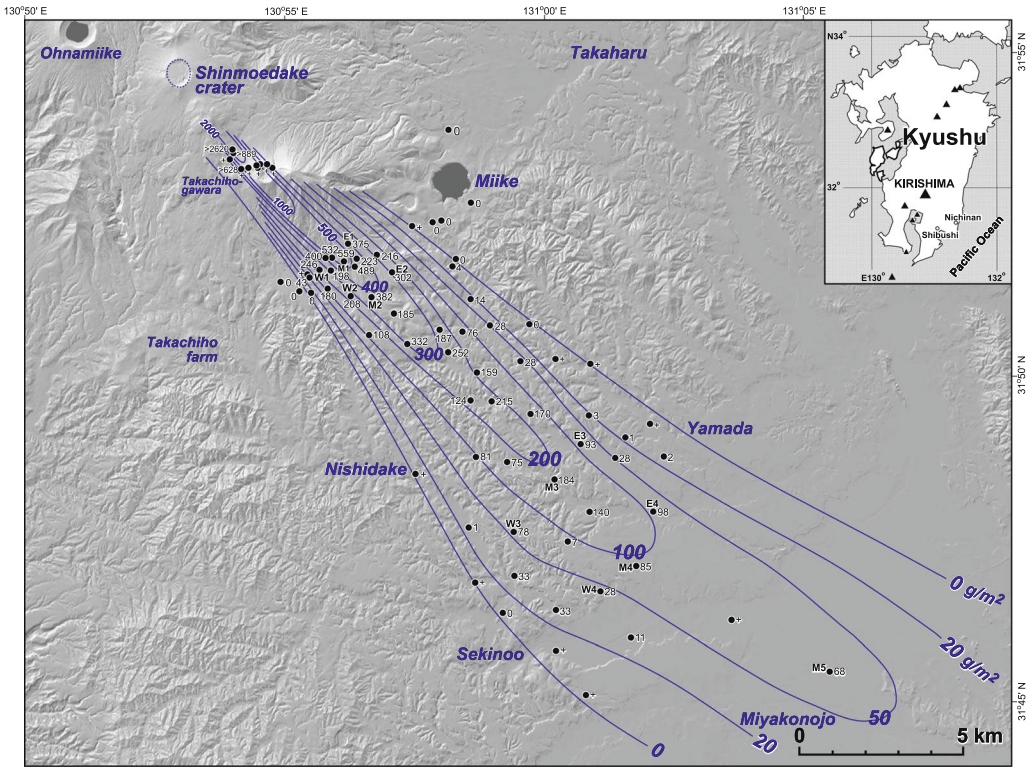

Fig. 2 Distribution map of the May 14, 2018, tephra fall deposit from the Shinmoedake crater, Kirishima Volcano. The relief map was produced by the Kashmir 3D software, using the 10-m-mesh digital elevation model (DEM) data published by the Geospatial Information Authority of Japan

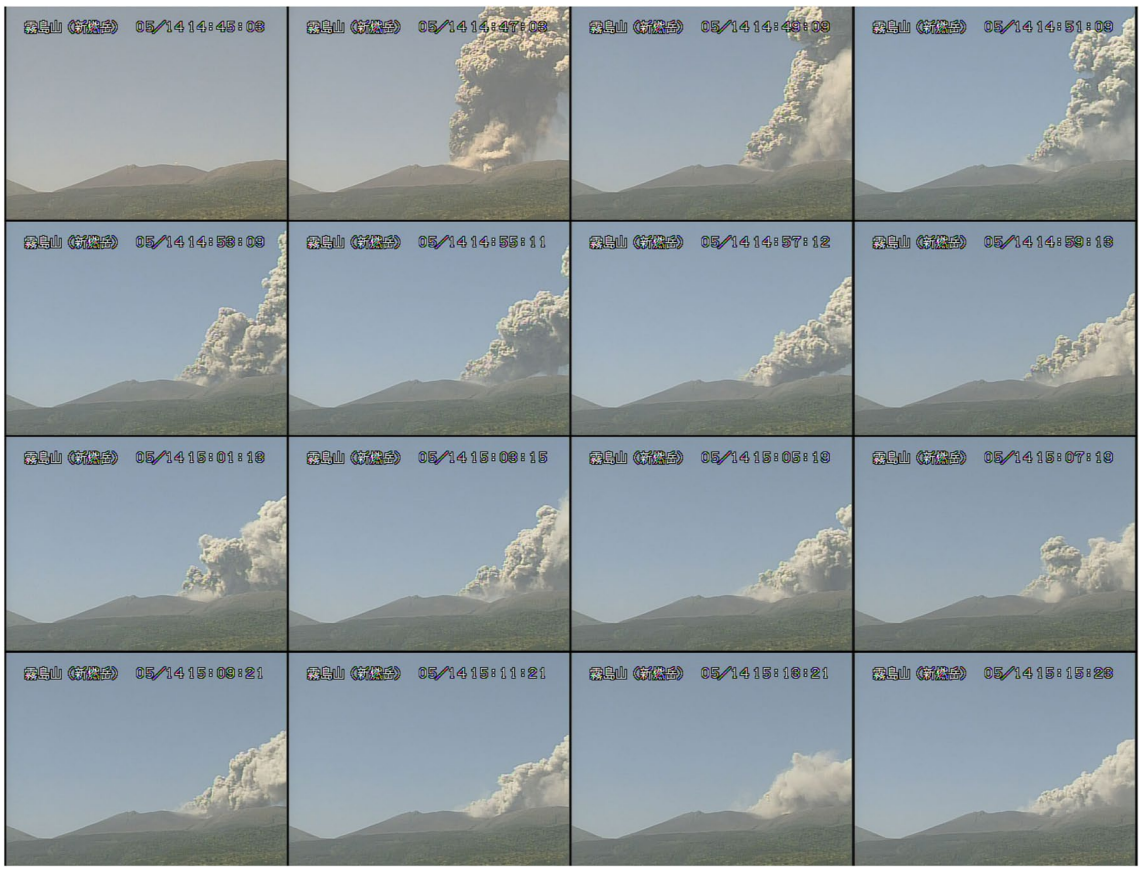

Fig. 3 Photographs of the May 14, 2018 eruption plume captured by the Japan Meteorological Agency (JMA) using camera installed at Inokoishi

The JMA installed several cameras to monitor the activity at Kirishima Volcano. Figure 1 portrays the layout of the surveillance cameras installed around the Shinmoedake crater. The May 14, 2018 eruption was captured using the cameras installed at Inokoishi and Karakunidake. In the photographs captured by the camera installed at Inokoishi (Fig. 3), a part of the plume was framed most of the time, but the entire plume was not captured. The camera installed at Karakunidake captured the entire plume from the upwind side of Shinmoedake (Fig. 4). Therefore, the camera at Karakunidake was predominantly used for photogrammetric analyses.

The JMA uses multiple numerical models to forecast daily atmospheric conditions and issue weather forecasts and warnings. In general, JMA uses the global spectral model (GSM) in their numerical models for global forecasts, meso-scale model (MSM) for forecasts for Japan, and local forecast model (LFM) for local forecasts. In this study, the vertical profile of the atmosphere over Shinmoedake was analyzed using meso-analysis (MA), which is the initial step of the MSM. As the horizontal resolution of the MA was 5 km, the wind data for the altitude directly above Shinmoedake were interpolated using the data from the surrounding grid.

Results

Distribution of tephra fall deposit and mass calculation

We created an isomass distribution map based on the field data (Fig. 2). The May 14, 2018 tephra-fall deposit was distributed southeast of the Shinmoedake crater. The dispersal axis extended approximately 16 km to the southeast and then, the direction changed slightly toward the east–southeast (Fig. 2). The northeastern dispersal limit was located near the line between the Shinmoedake crater and the Yamada office in Miyakonojo City. In contrast, our field survey revealed that the southwestern limit was located near the line between the Nishidake and Sekinoo. However, a road patrol company reported

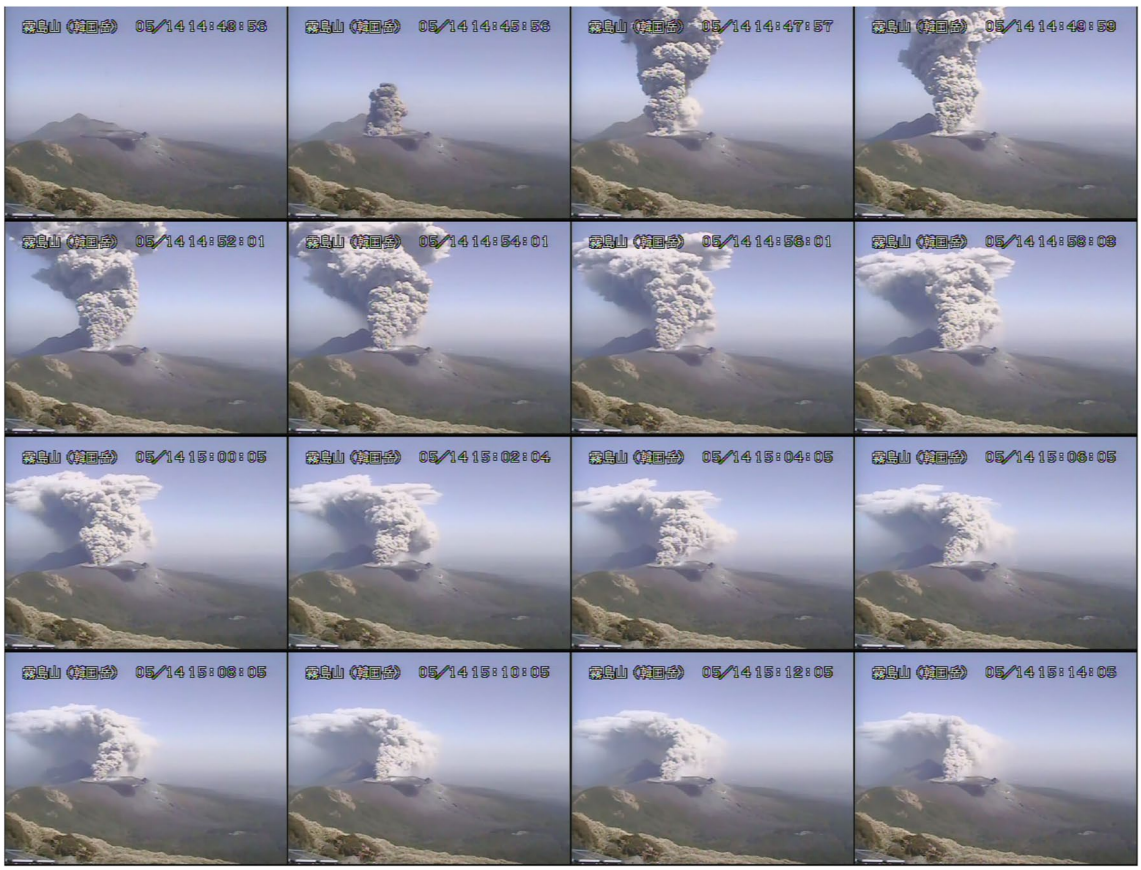

Fig. 4 Photographs of the May 14, 2018 eruption plume captured by the Japan Meteorological Agency (JMA) using camera installed at Karakunidake

seeing ash fall in more westerly locations, close to the Miyazaki and Kagoshima prefecture borders (such as Takachiho Farm in Fig. 2), suggesting that the ash fall was more widespread than estimated. The distal ash extended to Nichinan City (60 km SE) and Shibushi City (50 km SSE), along the Pacific coast following the southeast dispersal axis (Fig. 2) (Fukuoka Regional Headquarters and Kagoshima Meteorological Office 2019).

During our fieldwork on May 15 and 16, 2018, a maximum deposit mass of 559 g/m^2 was observed at a site approximately 7.3 km southeast of the source crater (Loc. M1; Fig. 5a); at this site, the ML was 7 mm. A deposit mass of more than 100 g/m^2 was observed approximately 20 km southeast of the crater. At the most distant observation site, approximately 26.1 km southeast of the crater (Loc. M5), the ash mass was 68 g/m^2, substantially greater than those observed at the adjacent observation sites (< 11 g/m^2). This was because the ash was well-preserved in the concave parts of the washboards (Fig. 5d). In contrast, 2 days after the eruption, most ash-fall deposits at other adjacent sites were blown.

We could not approach closer than 3 km to the Shinmoedake crater, owing to the risk of volcanic eruptions. On June 13, 2018, we conducted fieldwork in the area of Takachihogawara (~ 3 km S–SE of Shinmoedake), which is the base camp for the mountaineering expeditions to Kirishima Volcano. Although some of the tephra that erupted on May 14 was washed away by rain for almost a month after the eruption, a deposit mass greater than 2600 g/m^2 was observed at this site. The ML measured around Takachihogawara was 5–18 mm. The dispersal axis of ML was slightly more northeasterly than that of the isomass (Fig. 6).

By plotting the values of ten isomasses (2000, 1000, 500, 400, 300, 200, 100, 50, 20, and 0 g/m^2) on a distribution map (Fig. 2) we were able to calculate the entire eruptive mass of the May 14, 2018 tephra fall deposit. Figure 7 illustrates the relationship between each isomass' area and the deposit mass. In the proximal area, where the tephra deposit was more than 2000 g/m^2, we extrapolated a straight line connecting the isomass of 2000 g/m^2 with that of 1000 g/m^2 to the area of the

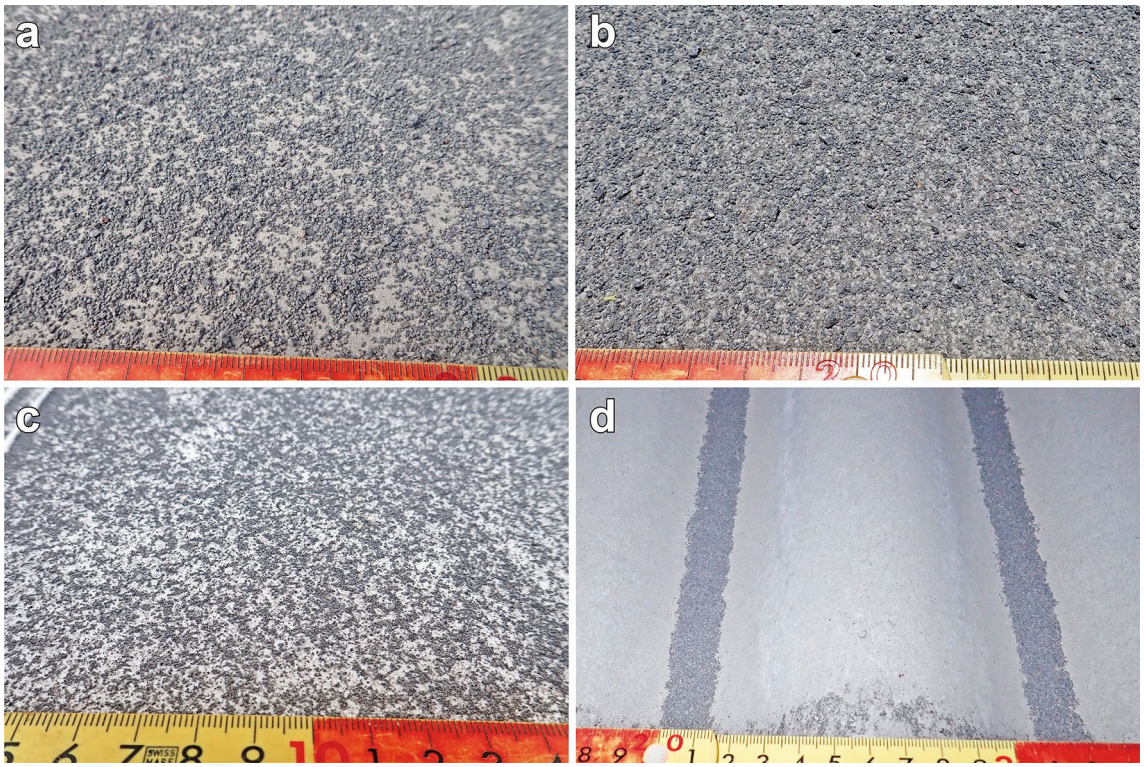

Fig. 5 Photographs of the May 14, 2018 tephra fall deposit from the Shinmoedake crater. **a** Coarse tephra fall deposit located 7.3 km southeast of the Shinmoedake crater (Loc. M1); image was captured at 16:20 on May 15, 2018. **b** Coarse tephra fall deposit located 8.6 km east–southeast of Shinmoedake crater (Loc. E2; image was captured at 11:55 on May 16, 2018). **c** Fine ash-fall deposit west of the main dispersal axis (Loc. W2; 8.2 km south–southeast of the crater); the photo was captured at 18:10 on May 15, 2018. **d** Ash-fall deposit at the most distant site located 26.1 km southeast of the crater (Loc. M5; image was captured at 19:30 on May 16, 2018). The scale is in centimeters. The locations of photographed sites are shown in Figs. 2 and 6

source vent (approximately 20 m in diameter). The mass–area relationship was divided into ten sections, and the mass in each section was calculated using integration. According to this method, the total mass of the May 14 tephra fall deposit was approximately 2.1×10^7 kg. Using the same isomass data and applying the two straight-line segments method proposed by Fierstein and Nathenson (1992), the total mass estimate is 2.1×10^7 kg, which is consistent with our result calculated by the trapezoidal-rule integration.

Characteristics of tephra fall deposits

The tephra fall deposits formed by the May 14, 2018 eruption were mainly gray lithic fragments found in the regions southeast of Shinmoedake Volcano. The deposit incidence varied with the dispersal direction (east–southeast to southeast and southeast to south–southeast of the source). The tephra deposits close to the main dispersal axis and east of the main axis were composed of coarse to medium sand-sized gray particles devoid of fine sand-to-silty grains (Fig. 5a, b). In contrast, the deposits west of the main dispersal axis were finer-grained (Fig. 5c) than the eastern deposits.

Digital microscopy observations revealed that the tephra fall deposits from the Shinmoedake crater that erupted on May 14, 2018, were predominantly lithic fragments with small amounts of free crystal grains (plagioclase, clinopyroxene, and orthopyroxene; typically < 2 mm in size) (Fig. 8). The lithic fragments were gray to dark gray, and most appeared fresh and glassy. These glassy lithic grains were thought to have originated from the fragments of dome lava that fill the Shinmoedake crater. There were no differences in the components of the tephra fall deposits along the different dispersal directions.

Grain size characteristics of deposits

The grain size distributions for all the samples were unimodal, with peaks observed at 1–2 ϕ (1/2–1/4 mm) or 0–1 ϕ (1–1/2 mm), irrespective of the distance from the crater or the dispersal direction (Fig. 9). The tephra deposits obtained within 8 km and 10 km were composed of particles finer than $-3\ \phi$ (< 8 mm) and $-2\ \phi$ (< 4 mm),

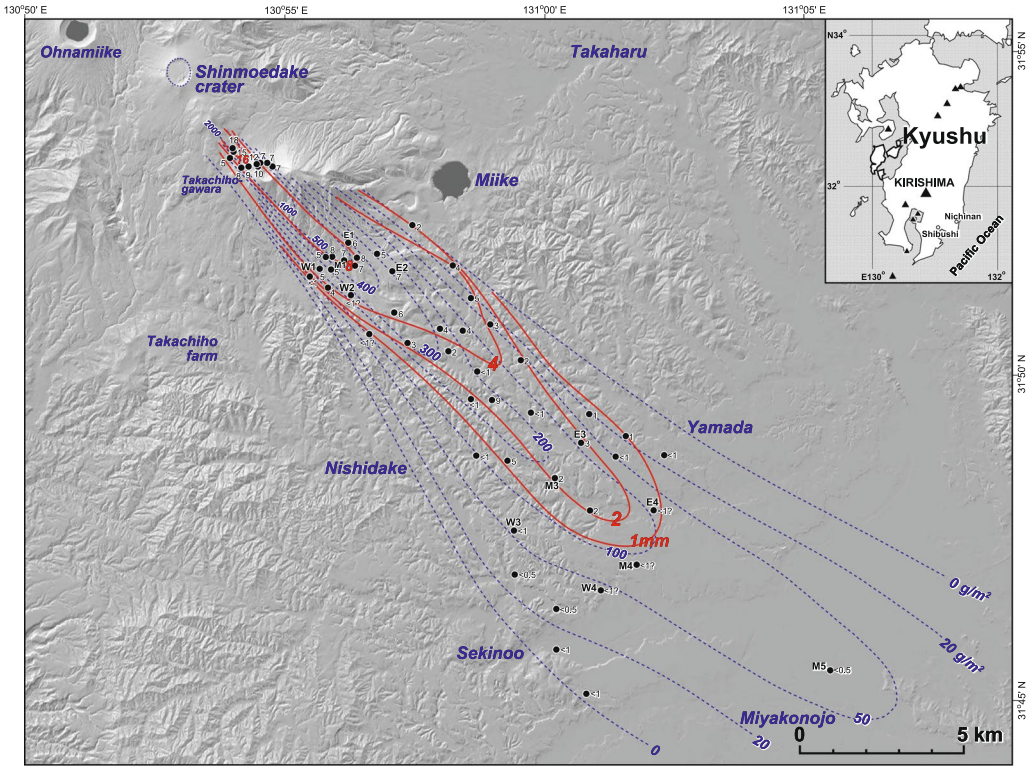

Fig. 6 Isopleth map of the May 14, 2018 deposit, with the maximum size of lithic fragments (ML; average long-axis diameter of the three largest lithic clasts at each locality) contained in the deposit. The relief map was produced by the Kashmir 3D software using the 10-m-mesh digital elevation model (DEM) data published by the Geospatial Information Authority of Japan

respectively. The distal deposit samples (> 15 km) were finer than 0 ϕ (< 1 mm). The Md_{ϕ} values increased with the distance from the crater (Figs. 9, 10), indicating that the tephra fall deposits that erupted on May 14 had increasingly finer grains at greater distances. The Md_{ϕ} values were substantially higher in the samples obtained from the west of the main dispersal axis than those obtained from the east of the axis. This indicates that the tephra samples obtained from the west of the main axis were finer grained than those obtained from the east of the axis. Overall, the tephra deposits were well-sorted (σ_{ϕ}: mostly < 0.8 ϕ). The sorting coefficients (σ_{ϕ}) did not vary over different distances or dispersal directions (Fig. 10).

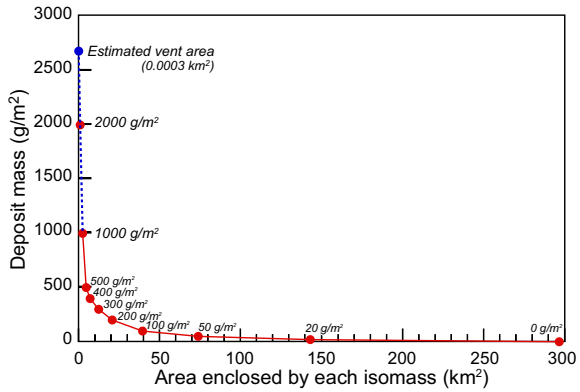

Fig. 7 Relationship between area (km^2) and mass (g/m^2) of the May 14, 2018 tephra fall deposit

Plume photogrammetry and meteorological data

Figure 4 portrays the temporal fluctuation of the eruption plume, as captured by the camera installed at Karakunidake; the top of the plume was out of frame immediately after the first vulcanian eruption. However, the plume's altitude dropped gradually; therefore, the entire plume remained in the frame. During the eruption, the plume flowed southeast (approximately 150°). The upper part of the plume flowed slightly eastward, while the lower part flowed slightly westward. These flow directions were constant throughout the eruption, as seen in the photographs shown in Fig. 4. The wind profile above the Shinmoedake crater (obtained from the metrological data) explains the difference in the flow direction.

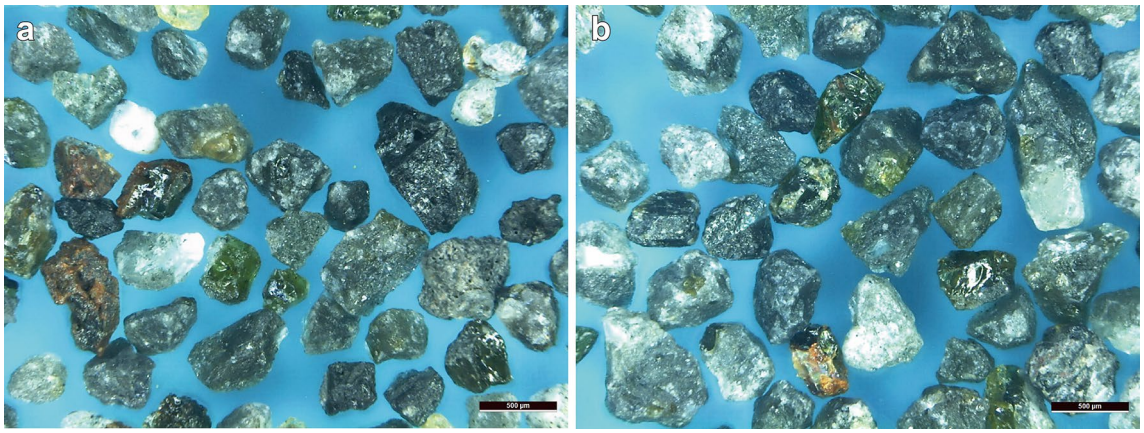

Fig. 8 Microphotographs of the ash grains (fraction 1–2 φ) of the May 14, 2018 tephra fall deposits sampled 8.2 km SSE (**a**; Loc. W2) and 8.6 km ESE (**b**; Loc. E2) of the Shinmoedake crater. The scale bar in the lower right of each photo is 500 μm

Figures 11 and 12 portray the wind direction profiles above Shinmoedake at 15:00 JST. The illustration shown in Fig. 12 is called a "hodograph" in meteorology. In a hodograph, a line connects the end points of the wind vector at each altitude. The wind vector's east–west component U [m/s] is on the X axis, while the north–south component V [m/s] is on the Y-axis. The curve displayed on the hodograph can be interpreted as the direction of elongation of a cumulonimbus cloud or volcanic plume as seen directly from above. The satellite image shown in Fig. 13 confirms this elongation direction.

The wind direction was 300°–315° in the upper part of the plume (2400–6000 m ASL), and 315°–325° in the lower part (below 2400 m ASL). As a result, the upper part advected east of the main axis, and the lower part advected west, as shown in the camera images. The Himawari meteorological satellite infrared image shown in Fig. 13 further demonstrates that the initial vulcanian eruption and the subsequent ash eruption were clearly separated. Furthermore, the ash eruption cloud can be divided into bright (east side) and dark (west side) regions, which correspond to the high and low regions of the plume, respectively.

Discussion

Estimation of total erupted mass

To estimate the total mass of the May 14, 2018 eruption deposit from Shinmoedake Volcano, we conducted a field survey immediately after the eruption (May 14–15, 2018), covering the area beyond 7 km southeast from the crater. We also carried out fieldwork in the proximal area (ca. 3–4 km southeast of the crater) on June 13, about 1 month after the eruption. In this section, we compare between erupted mass calculated using only distal data and calculations using both proximal and distal data (Table 1).

During the 2-day field survey after the May 14, 2018 eruption (May 15, 13:00–May 16, 19:30), we observed tephra fall deposits in areas located more than 7 km from the Shinmoedake crater. The largest deposit mass (559 g/m^2) was observed 7.3 km to the southeast of the crater, and the maximum isomass line that could be drawn was 500 g/m^2. Based on the relationship between the area enclosed by each isomass line and the mass of the deposit, the total erupted mass was estimated to be approximately 1.6×10^7 kg (Case 1 in Table 1). This value is about 80% of the total mass of 2.1×10^7 kg (Case 2), which was calculated using both the proximal (3–4 km southeast of the crater; obtained on June 13, 2018) and distal data (>7 km). Extrapolating a straight line connecting 500 g/m^2 with 400 g/m^2 to the area of the source vent (approximately 20 m in diameter), we estimated a tephra mass of 590 g/m^2 near the vent (Table 1), which was about one-fifth the tephra mass calculated from the survey results by including the proximal area (mass of approximately 2700 g/m^2; maximum isomass line: 2000 g/m^2).

The addition of the proximal data produced a difference in how the isomass lines were drawn, which produced differences in the areas enclosed by the isomass lines smaller than 500 g/m^2 (Table 1). The case in which the total mass of tephra fall deposits estimated for the distal area data was much smaller than that estimated for both proximal and distal area data was also reported in ash-fall surveys during the 2014–2015 eruptive activity that occurred at the Nakadake first crater, Aso Volcano (Miyabuchi and Hara 2019). Therefore, the tephra data for proximal areas is important to accurately estimate the mass of tephra fall deposits.

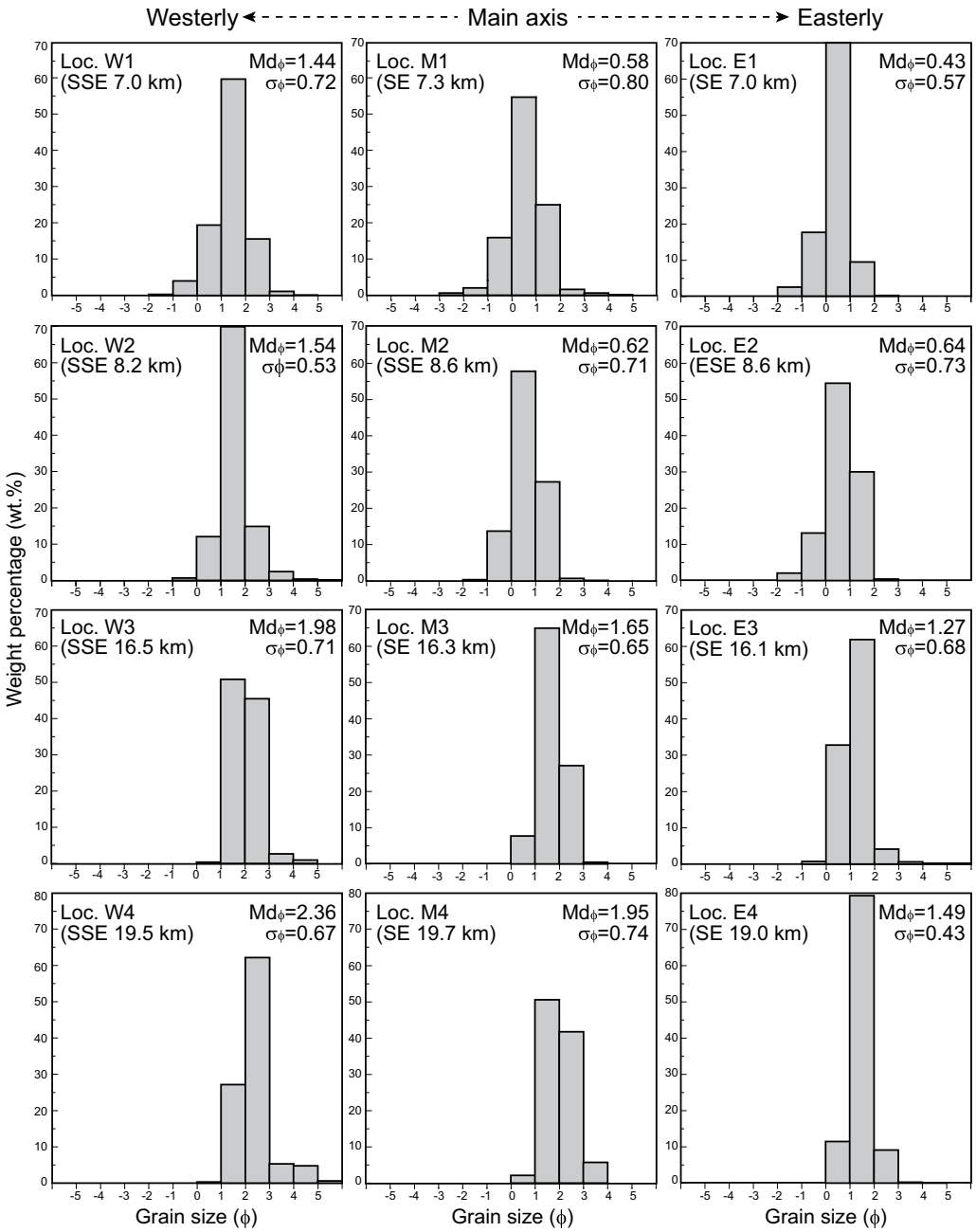

Fig. 9 Grain-size histograms for grains coarser than 5 φ (1/32 mm) of the representative samples of the tephra deposits. The locations of the sampling sites are shown in Figs. 2 and 6

Sequence of the May 14, 2018 eruption

The May 14, 2018 eruption at the Shinmoedake crater, Kirishima Volcano, produced tephra fall deposits that were distributed more than 27 km southeast of the source crater; these deposits have a mass of approximately 2.1×10^7 kg. The deposits are mainly composed of fresh glassy lithic fragments, probably derived from the dome lava inside the crater. The component characteristics of the deposits are comparable to those of the vulcanian eruptions of March 2011 (Miyabuchi et al. 2013). Therefore, the May 14, 2018 Shinmoedake eruption was accompanied by a vulcanian explosion. This is consistent with the photographic records obtained by the JMA (Figs. 3, 4).

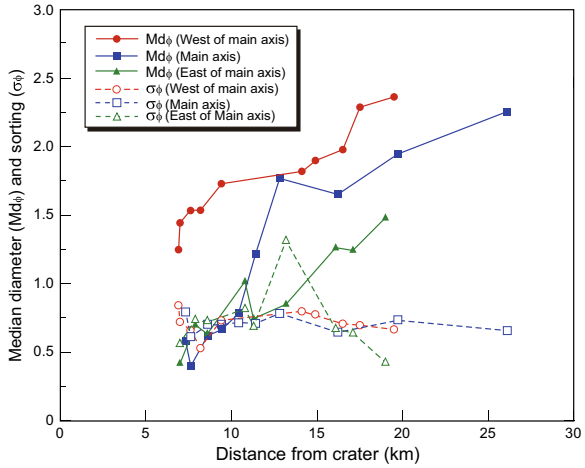

Fig. 10 Relationship between median diameters (Md_{ϕ}) and the Inman (1952) sorting coefficients (σ_{ϕ}) for the May 14, 2018 tephra-fall deposits and their distance from the Shinmoedake crater

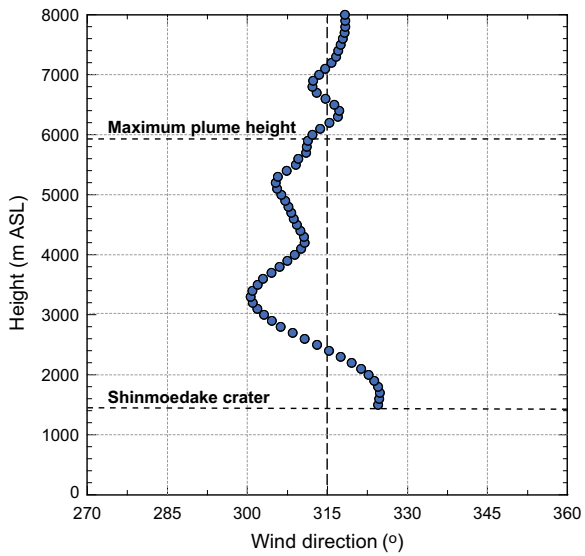

Fig. 11 Vertical distribution of wind direction above the Shinmoedake crater at 15:00 JST on May 14, 2018, deduced by the Japan Meteorological Agency (JMA) using meso-analysis (MA)

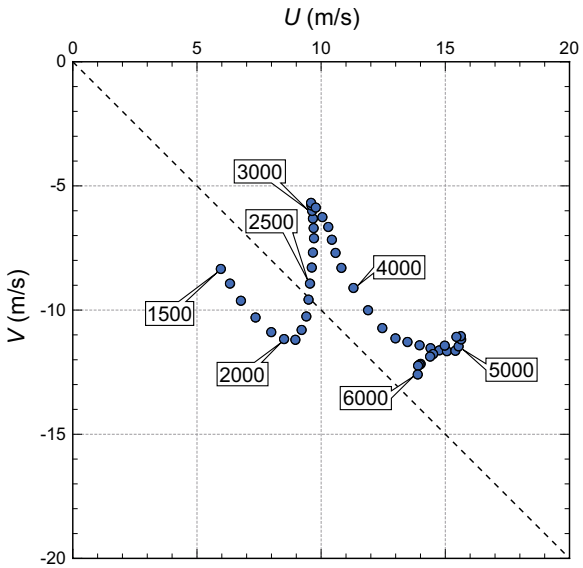

Fig. 12 Hodograph portraying the wind direction above the Shinmoedake crater at 15:00 JST on May 14, 2018. U (> 0) and V (< 0) represent westerly and northerly components of the wind, respectively. Numbers inside balloons indicate the altitude above sea level (m ASL)

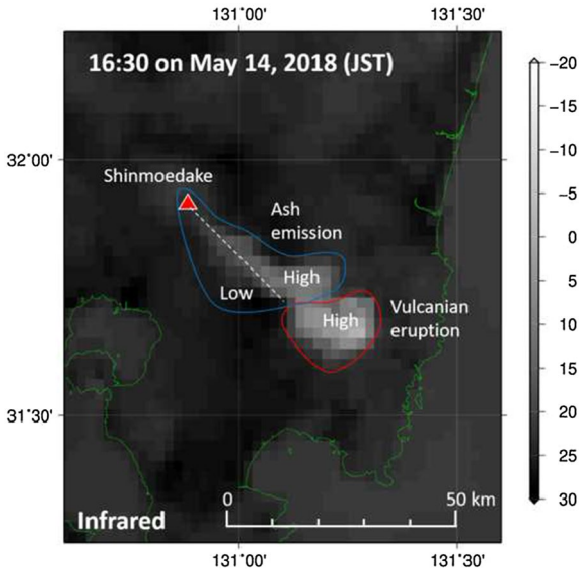

Fig. 13 Infrared image captured by the Himawari-8 meteorological satellite at 16:30 JST on May 14, 2018. Lower brightness temperature indicates higher altitude

The grain size characteristics of the tephra fall deposits on the east and west sides of the main axis differed significantly. The deposits on the east side of the main axis consisted of relatively coarser particles and had larger ML values. In contrast, the deposits on the west side were composed of finer grains and had smaller ML values. These features can be explained by the eruption stage and the vertical wind profile over the Shinmoedake crater (Figs. 11, 12, 14).

A vulcanian eruption occurred during the first stage of the May 14, 2018 eruption, transporting relatively coarse particles to the upper part of the plume. These particles were advected by the wind blowing at approximately 2400–6000 m ASL. The wind direction at this

Table 1 Mass of tephra discharged and isomass area for each survey case for the May 14, 2018 eruption deposit analyzed in this study

Case	Case 1		Case 2	
Used data	Distal (> 7 km) data		Proximal (3–4 km) and distal (> 7 km) data	
	Mass (g/m^2)	Area (km^2)	Mass (g/m^2)	Area (km^2)
Mass in vent area	592	0.0003	2683	0.0003
Drawn isomass and area			2000	1.0301
			1000	2.5383
	500	2.5288	500	4.7316
	400	5.2835	400	7.0755
	300	10.8938	300	12.3822
	200	19.5572	200	20.8152
	100	38.6822	100	39.4625
	50	72.7971	50	73.9510
	20	141.3119	20	143.1269
	0	296.4031	0	297.1475
Calculated mass (kg)		1.6×10^7		2.1×10^7

The mass in the source vent area was estimated by extrapolating the straight line that connects the maximum isomass with the second maximum isomass to the area of the source vent (approximately 20 m in diameter)

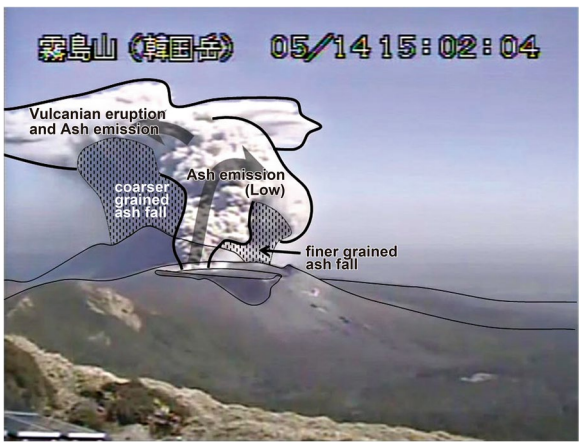

Fig. 14 Schematic illustration of the relationship between the May 14, 2018 eruptions and the properties of ash-fall, based on the photo captured by the Japan Meteorological Agency (JMA), using the camera installed at Karakunidake, and the ambient wind field data

height was 300°–315°; below 2400 m ASL, the wind direction was 315°–325°. Because of this variation in the wind direction, the coarse particles from the upper part of the plume were deposited only on the east side of the main axis, and the fine particles from the lower part of the plume were deposited on the west side of the main axis. Consequently, the percentage of relatively coarse particles was high on the east side.

During the later phase, the particles from the ash emission plume were primarily deposited on the west side of the main axis because in this phase, the plume's height was lower than 2400 m. The tephra segregation height decreased with the plume altitude; however, the sorting coefficients of the deposits sampled from the east and west of the main axis did not portray remarkable differences.

The satellite image (Fig. 13) also shows that parts of the ash emission and initial vulcanian eruption plumes rose to a high altitude, although the particles inside the ash emission plume were considered to be fine-grained. Consequently, on the east side of the main axis, only the coarse-grained particles associated with the vulcanian eruption were deposited in the proximal area (< 15–20 km from the crater).

To the best of our knowledge, this study is the first to explore vertical wind shear and its influence on volcanic eruption plumes. Previous plume modeling studies rarely consider vertical wind shear. However, as plume dynamics models will be extended to three dimensions in the future, the consideration of vertical wind shear is unavoidable. Few previous ash-fall simulations considered the influence of vertical wind shear (for example, Mannen et al. 2020). Incorporating the influence of vertical shear to current ash fall simulations can allow for more accurate reconstructions of tephra distributions, although this would require extensive discussions using real-world cases, as in this study. An accurate reconstruction of the vertical profile of volcanic ash inside the plume, as considered in previous studies (Mannen 2014; Connor et al. 2019; Mannen et al. 2020), involves resolving an inverse issue. The findings of this study can be

combined with earlier works to yield useful information regarding the vertical profile of volcanic ash particles in the atmosphere.

Conclusions

For this study, the spatial distribution and grain-size characteristics of the tephra fallout deposits that erupted from the Shinmoedake crater (Kirishima Volcano) on May 14, 2018 were investigated immediately after the eruption. The tephra fall deposits were dispersed more than 27 km southeast of the crater, and the total mass was estimated to be approximately 2.1×10^7 kg, based on an isomass map. We noted differences between the deposits on the east and west sides of the main dispersal axis. The deposits observed on the east side were composed mainly of coarse to medium sand-sized particles, whereas the deposits on the west side were finer grained than those on the east side. Based on the photographs of the eruption plume and the meteorological data, we theorized the cause of these differences. According to meteorological data, the wind direction over the Shinmoedake crater during the eruption varied with altitude. The upper part of the plume associated with the first vulcanian eruption spread east of the main axis, catching the westerly winds. As a result, the relatively coarse-grained tephra was deposited on the east side of the axis. In contrast, the subsequent ash emission plume dispersed west of the main axis, due to northerly winds, and the ash (consisting of relatively finer particles) was deposited on the west side of the axis. As the plume altitude of the ash eruption decreased gradually, there was a change in the segregation altitude of the fine-grained particles, resulting in finer-grained tephra being deposited on the western side of the main axis.

This study demonstrates that the spatial and grain-size distributions of the tephra fall deposits associated with an eruption can generally be explained by the eruption style and vertical wind profile over the source volcano. However, it is necessary to solve the inverse problem to accurately reconstruct the vertical profile of the volcanic ash plume in the atmosphere. Such analyses can provide useful information regarding the vertical profiles of ash particles inside volcanic plumes. This information can improve the current plume analysis methods carried out using weather radars and dispersion forecasts carried out using numerical models.

Abbreviations

ASL	Above sea level
DEM	Digital elevation model
GSM	Global spectral model
JMA	Japan Meteorological Agency
JST	Japan Standard Time
LFM	Local forecast model
MA	Meso-analysis
Md_φ	Median diameters
ML	Maximum size of lithic fragments
MSM	Meso-scale model
PDC	Pyroclastic density current

Supplementary Information

The online version contains supplementary material available at https://doi.org/10.1186/s40623-023-01907-3.

Additional file 1. Table S1: Field data for the mass loadings and the maximum sizes of lithic grains in the samples of tephra deposit analyzed in this study.

Additional file 2. Table S2: Grain size characteristics of the tephra deposits of the Shinmoedake eruption that occurred on May 14, 2018.

Acknowledgements

Ash sampling and grain-size analysis were supported by Yusuke Arakawa and Nami Sasai, respectively. Daiken Co., Ltd. (a road patrol company in Miyakonojo City) provided valuable information about the eruption column and the tephra fall conditions. We thank the Kagoshima Meteorological Office (Japan Meteorological Agency) for providing the operational camera data. The manuscript was improved through constructive comments from two anonymous reviewers. We also acknowledge the editorial assistance provided by Takayuki Kaneko.

Author contributions

YM carried out the field survey, tephra sampling, data processing, drawing of the distribution maps, calculation of the discharged masses, and grain size analysis of the tephra fall deposits. ES analyzed the meteorological data and photographs. All the authors have read and approved the final version of the manuscript.

Funding

Not applicable.

Availability of data and materials

The data sets used and analyzed in the current study are available from the corresponding author upon reasonable request.

Declarations

Ethics approval and consent to participate

Not applicable.

Consent for publication

Not applicable.

Competing interests

The authors declare that they have no competing interests.

Author details

[1]Center for Water Cycle, Marine Environment and Disaster Management, Kumamoto University, Kurokami 2-39-1, Chuo-ku, Kumamoto 860-8555, Japan. [2]Meteorological Research Institute, Japan Meteorological Agency, 1-1 Nagamine, Tsukuba, Ibaraki 305-0052, Japan.

Received: 2 April 2023 Accepted: 23 September 2023
Published online: 05 December 2023

References

Connor CB, Connor LJ, Bonadonna C, Luhr J, Savov I, Navarro-Ochoa C (2019) Modelling tephra thickness and particle size distribution of the 1913 eruption of Volcán de Colima, Mexico. Volcán de Colima: Portrait of a Persistently Hazardous Volcano. Springer, London, pp 81–110

Fierstein J, Nathenson M (1992) Another look at the calculation of fallout tephra volumes. Bull Volcanol 54:156–167. https://doi.org/10.1007/BF00278005

Fukuoka Regional Headquarters, Kagoshima Meteorological Office (2018) Volcanic Regular Bulletin of Kirishima Volcano in 2017, p 61 (**in Japanese**)

Fukuoka Regional Headquarters, Kagoshima Meteorological Office (2019) Volcanic Regular Bulletin of Kirishima Volcano in 2018, p 92 (**in Japanese**)

Hashimoto A, Shimbori T, Fukui K (2012) Tephra fall simulation for the eruptions at Mt. Shinmoe-dake during 26–27 January 2011 with JMANHM. Sola 8:37–40. https://doi.org/10.2151/sola.2012-010

Imura R (1994) Geology of Kirishima volcano. Bull Earthq Res Inst Univ Tokyo 69:189–209 (**in Japanese with English abstract**)

Imura R, Kobayashi T (2001) Geological map of Kirishima Volcano (1:50,000). Geological map of volcanoes 11. Geological Survey of Japan (**in Japanese with English abstract**)

Imura R, Koga M (1992) ^{14}C-ages of charcoal from the Kirishima Volcano and the Ito Ignimbrite. Bull Volcanol Soc Jpn 37:99–102 (**in Japanese**)

Inman DL (1952) Measures of describing the size distribution of sediments. J Sedim Petrol 22:125–145

Inoue K (1988) The growth history of Takachiho composite volcano in the Kirishima volcano group. J Min Petrol Econ Geol (ganko) 83:26–41 (**in Japanese with English abstract**)

Kozono T, Ueda H, Ozawa T, Koyaguchi T, Fujita E, Tomiya A, Suzuki YJ (2013) Magma discharge variations during the 2011 eruptions of Shinmoe-dake volcano, Japan, revealed by geodetic and satellite observations. Bull Volcanol 75:695. https://doi.org/10.1007/s00445-013-0695-4

Maeno F, Shohata S, Suzuki Y, Hokanishi N, Yasuda A, Ikenaga Y, Kaneko T, Nakada S (2023) Eruption style transition during the 2017–2018 eruptive activity at the Shinmoedake volcano, Kirishima, Japan: Surface phenomena and eruptive products. Earth Planets Space 75:76. https://doi.org/10.1186/s40623-023-01834-3

Mannen K (2014) Particle segregation of an eruption plume as revealed by a comprehensive analysis of tephra dispersal: theory and application. J Volcanol Geotherm Res 284:61–78. https://doi.org/10.1016/j.jvolgeores.2014.07.009

Mannen K, Hasenaka T, Higuchi A, Kiyosugi K, Miyabuchi Y (2020) Simulations of tephra fall deposits from a bending eruption plume and the optimum model for particle release. J Geophys Res Solid Earth 125(JB018902):e2019. https://doi.org/10.1029/2019JB018902

Miyabuchi Y, Hara C (2019) Temporal variations in discharge rate and component characteristics of tephra-fall deposits during the 2014–2015 eruption of Nakadake first crater, Aso Volcano. Japan. Earth Planets Space 71:44. https://doi.org/10.1186/s4062

Miyabuchi Y, Hanada D, Niimi H, Kobayashi T (2013) Stratigraphy, grain-size and component characteristics of the 2011 Shinmoedake eruption deposits, Kirishima Volcano, Japan. J Volcanol Geotherm Res 258:31–46. https://doi.org/10.1016/j.jvolgeores.2013.03.027

Nakada S, Nagai M, Kaneko T, Suzuki Y, Maeno F (2013) The outline of the 2011 eruption at Shinmoe-dake (Kirishima), Japan. Earth Planets Space 65:475–488. https://doi.org/10.5047/eps.2013.03.016

Poulidis AP, Phillips JC, Renfrew IA, Barclay J, Hogg A, Jenkins SF, Robertson R, Pyle DM (2018) Meteorological controls on local and regional volcanic ash dispersal. Sci Rep 8:6873. https://doi.org/10.1038/s41598-018-24651-1

Sato E (2021) Kusatsu-Shirane volcano eruption on January 23, 2018, observed using JMA operational weather radars. Earth Planets Space 73:117. https://doi.org/10.1186/s40623-021-01445-w

Sato E, Fukui K, Shimbori T (2018) Aso volcano eruption on October 8, 2016, observed by weather radars. Earth Planets Space 70:105. https://doi.org/10.1186/s40623-018-0879-4

Shimbori T, Sakurai T, Tahara M, Fukui K (2013) Observation of eruption clouds with weather radars and meteorological satellites: a case study of the eruptions at Shinmoedake volcano in 2011. Q J Seismol 77:139–214 (**in Japanese**)

Walker GPL (1983) Ignimbrite types and ignimbrite problems. J Volcanol Geotherm Res 17:65–88. https://doi.org/10.1016/0377-0273(83)90062-8

Publisher's Note